Industrial Crops & Products 182 (2022) 114951

Contents lists available at ScienceDirect

Industrial Crops & Products

journal homepage: www.elsevier.com/locate/indcrop

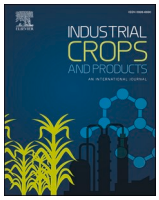

Guayulin content, resin and rubber fraction by near infrared spectroscopy in guayule stems (Parthenium argentatum, A. Gray)

M. Mercedes García-Martínez [a], Guayente Latorre [a], Francisco Miguel Jara [b], Juana Rozalén [a], M. Engracia Carrión [c,1], Manuel Carmona [c], Amaya Zalacain [a,*]

[a] Universidad de Castilla-La Mancha, Cátedra de Química Agrícola, Escuela Técnica Superior de Ingenieros Agrónomos y de Montes, Campus Universitario s/n, 02071 Albacete, Spain
[b] Instituto Técnico Agronómico Provincial (ITAP) S.A. Polígono Industrial Campollano, Avenida 2, 42 B, 02007 Albacete, Spain
[c] Universidad de Castilla-La Mancha, Institute for Regional Development (IDR), Food Quality Research Group, 02071 Albacete, Spain

ARTICLE INFO

Keywords:
Guayule
Resin
Rubber
Guayulins
Near infrared spectroscopy
Partial least squares regression model

ABSTRACT

Guayule (*Parthenium argentatum*, A. Gray) is a promising alternative source to natural rubber from *Hevea brasiliensis* L. Recently, another important fraction of its composition, the resin, has been the focus of many studies due to its promising commercial applicability. In the resin extract there are guayulins (A, B, C and D), belonging to the sesquiterpene family, which are usually analyzed by HPLC-DAD and, lately, with other labor-intensive analytical techniques. Near infrared spectroscopy (NIR) has been successfully used in fresh guayule and dry biomass to assess moisture, and total rubber and resin content. The purpose of the present study is to estimate, for the first time ever, the detailed guayulin content in guayule dry stems using NIR spectroscopy. So, a set of 144 samples were analyzed by a Perkin Elmer Spectrum One FT-NIR equipment coupled with a near infrared reflectance accessory (NIRA). In addition, guayulins A and B standards, isolated in the lab, were scanned to generate the best partial least squares regression (PLSR) model. The best correlative PLSR models for resin, rubber and guayulins were developed within the range of 1100–2500 nm, showing an excellent calibration correlation (r^2c = 0.92–1.00) and cross validation (r^2cv = 0.87–0.92). The residual predicative deviation (RPD) was above 3 in the case of resin, rubber and guayulins A, B and D; while in guayulin C was 2.8. These high RPD values demonstrated a good prediction power of the model. In conclusion, the use of NIR spectroscopy for the estimation of resin and guayulin content in ground guayule stems is an excellent option for the routine analysis instead of time-consuming and labor-intensive traditional techniques.

1. Introduction

Guayule (*Parthenium argentatum*, A. Gray) is the most promising alternative source to natural rubber from *Hevea brasiliensis*. But it has another important chemical fraction containing many identified terpenoid compounds (Cheng et al., 2020; Jara et al., 2019; Rozalén et al., 2021d), as well as fatty acid triglycerides, lipids, pigments, inulin and other acetone-soluble materials (Banigan et al., 1982; Salvucci et al., 2009).

The isolation/extraction of both the rubber and resin fractions in guayule tissue is performed by solid-liquid extraction using organic solvents (Coffelt et al., 2009; Salvucci et al., 2009). The accelerated solvent extraction (ASE) quantification method is the most commonly used technique, and rubber and resin yields are gravimetrically determined (Cornish et al., 2013; Rozalén et al., 2021a; Schloman et al., 1983; Suchat et al., 2013). Once the main resin or rubber fractions have been extracted, various analytical procedures were used to quantify their compositions (Angulo-Sánchez et al., 1995; Cheng et al., 2020; McMahan et al., 2006; Romo de Vivar et al., 1990; Rozalén et al., 2021d; Spano et al., 2018).

Nowadays, there has been a before and after in the routine control of different products with the introduction of spectroscopic techniques such as near infrared spectroscopy (NIR), which is based on the vibrational properties of the organic molecules chemical bonds and their

* Corresponding author.
E-mail addresses: Mariamercedes.Garcia@uclm.es (M.M. García-Martínez), Guayente.Latorre@uclm.es (G. Latorre), fjg.itap@dipualba.es (F.M. Jara), Juana.Rozalen@uclm.es (J. Rozalén), Manuel.Carmona@uclm.es (M. Carmona), Amaya.Zalacain@uclm.es (A. Zalacain).
[1] MEngracia.carrión@uclm.e

https://doi.org/10.1016/j.indcrop.2022.114951
Received 30 December 2021; Received in revised form 11 April 2022; Accepted 12 April 2022

Table 1
Comparison of the studies carried out on guayule using NIR spectroscopy.

Parameters	Black et al. (1985)	Suchat et al. (2013)	Taurines et al. (2019)	Luo et al. (2019)
Title of article	Analysis of rubber, resin and moisture content of guayule by near infrared reflectance spectroscopy	Fast determination of the resin and rubber content in *Parthenium argentatum* biomass using near infrared spectroscopy	Determination of natural rubber and resin content of guayule fresh biomass by near infrared spectroscopy	A high-throughput quantification of resin and rubber contents in *Parthenium argentatum* using near-infrared (NIR) spectroscopy
Number of samples	110 samples	215 samples	200 samples	315 samples
Type of samples	1–2 cm ground dried guayule biomass	< 0.5 mm ground dried guayule biomass	Powders, dry branches, and fresh branches	2 mm ground dried guayule biomass
Chemical method of analysis	Polytron	Soxhlet Polytron PT 3100 homogenizer ASE Dionex Model 350	ASE Dionex Model 350	ASE Dionex Model 200
Range of contents	Resin (%): 1.50–11.00 Rubber (%): 0.80–19.00	Resin (%): 3.27–13.42 Rubber (%): 0.74–13.81	Resin (%): 5.35–10.68 Rubber (%): 2.65–9.21	Resin (%): 5.85–21.03 Rubber (%): 0.61–9.68
NIR instrument	Neotec Model 6350 Mark II	Foss XDS monochromator	ASD Portable spectrometer LabSpec 4 Standard-Res	ASD FieldSpec®3 spectrophotometer Handheld Polychromix Phazir™ 1624
Scanning range	1100–2500 nm	400–2500 nm	800–2400 nm	ASD FieldSpec®3: 750–2500 nm Polychromix Phazir™: 1600–2400 nm
Wavelengths of resin and rubber	Resin: 1708/2388/2170 nm Rubber: 1716/2208/2322 nm	Resin and rubber: 1708/1716/2210/2308	Resin: 970 nm Resin and rubber: 1150/1215/1740/1780/2260/2315 nm	Resin: 1184/1385/1668/1690/1886/1914/2248/2278/2297/2324 nm Rubber: 1205/1389/1410/1686/1716/1736/1781/1883/1914/2260 nm
NIR equations resin[a, b, c, d, e, f, g, h]	$r^2c = 0.85$	$r^2c = 0.96$; $r^2p = 0.96$; RPDc = 4.23; RPDp = 4.80	Powders: $r^2c = 0.95$; $r^2cv = 0.84$; $r^2p = 0.83$; RMSEC = 0.21; RMSECV = 0.37; RMSEP = 0.34 Dry branches: $r^2c = 0.56$; $r^2cv = 0.49$; $r^2p = 0.47$; RMSEC = 0.62; RMSECV = 0.67; RMSEP = 0.67 Fresh branches: $r^2c = 0.55$; $r^2cv = 0.41$; $r^2p = 0.38$; RMSEC = 0.63; RMSECV = 0.73; RMSEP = 0.75	DRY (water-stressed): $r^2cv = 0.82$; $r^2p = 0.83$; RPDp = 2.41; RMSEC = 1.07; RMSECV = 1.23; RMSEP = 1.20 IRR (non-stressed): $r^2cv = 0.69$; $r^2p = 0.77$; RPDp = 2.07; RMSEC = 1.51; RMSECV = 1.55; RMSEP = 1.34 DRY+IRR: $r^2cv = 0.73$; $r^2p = 0.76$; RPDp = 2.05; RMSEC = 1.57; RMSECV = 1.59; RMSEP = 1.49
NIR equations rubber	$r^2c = 0.99$	$r^2c = 0.98$; $r^2p = 0.96$; RPDc = 5.28; RPDp = 4.58	Powders: $r^2c = 0.97$; $r^2cv = 0.96$; $r^2p = 0.95$; RMSEC = 0.28; RMSECV = 0.33; RMSEP = 0.31 Dry branches: $r^2c = 0.83$; $r^2cv = 0.78$; $r^2p = 0.71$; RMSEC = 0.64; RMSECV = 0.72; RMSEP = 0.84 Fresh branches: $r^2c = 0.73$; $r^2cv = 0.71$; $r^2p = 0.75$; RMSEC = 0.79; RMSECV = 0.83; RMSEP = 0.79	DRY (water-stressed): $r^2cv = 0.76$; $r^2p = 0.78$; RPDp = 2.13; RMSEC = 0.66; RMSECV = 0.76; RMSEP = 0.72 IRR (non-stressed): $r^2cv = 0.73$; $r^2p = 0.75$; RPDp = 2.02; RMSEC = 0.60; RMSECV = 0.68; RMSEP = 0.65 DRY+IRR: $r^2cv = 0.73$; $r^2p = 0.76$; RPDp = 2.02; RMSEC = 0.73; RMSECV = 0.79; RMSEP = 0.75

[a] r^2c: coefficient of determination for calibration; [b] r^2p: coefficient of determination for prediction; [c] r^2cv: coefficient of determination for cross validation; [d] RPDc: ratio performance to deviation; [e] RPDp: ratio performance to deviation for prediction; [f] RMSEC: root mean squared error of calibration; [g] RMSECV: root mean squared error of cross validation; [h] RMSEP: root mean squared error of prediction.

interactions with NIR radiation. It is a technique used for rapid, reliable, and non-destructive prediction of chemical components in plants (Wang et al., 2021; Xiao et al., 2014). The feasibility of NIR spectroscopy may include, but it is not limited to, the determination of a suitable NIR response. Establishing a reliable and robust PLSR model is a critical procedure for the successful application of NIR, and many parameters should be optimized (Zhao et al., 2015) including spectral pretreatment, variable selection and latent factors. The NIR spectra also show unexpected chemical interferences and, even when it is not likely to list all variables, these may include the environmental measurement conditions, like sample temperature, residual moisture and solvents, sample particle size, homogeneity, and the age of samples, among others.

The NIR spectroscopy has been successfully used on fresh ground guayule and dry biomass to assess moisture, and total rubber resin content, as shown in Table 1.

Differences among previous studies may be attributed to several factors (Table 1), and the most significant differences were observed considering the sample preparation, as the number of samples tripled between studies, ranging from 110 to 315, and the sample particle size varied from 0.5 mm to 2 cm. The accelerated solvent extraction (ASE) is the technique used for resin and rubber determination in all papers, except for Black et al. (1985). Only Taurines et al. (2019) assessed rubber and resin on the whole fresh and dry biomass and ground samples. Although the standard error of prediction was two times higher for fresh and dry biomass than for ground samples, it was a good approach to determinate the average content of the plot before harvest. There are also differences among NIR instruments, spectral ranges and resolution, but only Luo et al. (2019) attempted comparison between different NIR equipment and scanning range. The calibration method performed in all studies agrees to PLSR models and their prediction accuracy obtained for estimating rubber and resin total content for guayule accessions are considered better than satisfactory.

There is only one paper referred to guayule latex quantification by NIR (Cornish et al., 2004) with strong correlations between measured and predicted rubber concentration. Although there are differences between an homogenate guayule latex sample and purified latex due to the presence of other soluble plant components, such as resin and proteins, that fact does not interfere when rubber quantification is carried out.

In order to enhance the economic viability of guayule as an industrial crop, value-added uses for the resin fraction (Dehghanizadeh et al., 2021; Jara et al., 2019) and residues (Cheng et al., 2020) are needed to achieve the gross rubber production costs reduction. In case of guayule resin, it has been reported to have antifungal, insect antifeedant and wood protector activities attributed in some cases to the sesquiterpene

Table 2
Guayule accessions, growth stage, and number of samples studied.

Germplasm	Species	Origin/Year	Nº Samples	Growth Stage (months)
CAL-1	*P. argentatum* Gray *x P. tomentosum var. tomentosum DC*	USDA-CA (1982)	48	*6, 12, 18, and 23*
AZ-2	Hybrid guayule x unknown	USDA-AZ (1997)	48	
R-1040	*P. argentatum*	Coahuila, México (1976)	48	

fraction compounds, known as guayulins (Bultman et al., 1991; Maatooq, 2002; Maatooq and Hoffmann, 1996; Nakayama et al., 2001). They could be exploited as biopesticides (fungicides, insecticides and miticides) or as starting material for semi-synthesis of other compounds may also be of interest to chemical and pharmaceutical companies (Jara et al., 2019). The guayulin content of guayule is known to change along the growth cycle and the crop management (Coffelt and Williams, 2009; Rozalén et al., 2021b, 2021c; Schloman et al., 1996, 1986), and even some authors suggested that guayulins may be involved in the synthesis of natural rubber (Rozalén et al., 2021c, 2021b) opening a new avenue to explore their possible contribution in the future.

Guayulins have been determined by the most commonly used analysis method, HPLC-DAD (Martínez et al., 1986; Rozalén et al., 2021d; Schloman et al., 1983; Spano et al., 2018; Teetor et al., 2009) and more recently with other analytical techniques including LC-MS, ESI-TOF, and MALDI-TOF (Rozalén et al., 2021d). The introduction of these techniques in the routine analysis of guayulins is not always possible due to the equipment cost, but NIR could serve as a quick and versatile tool for routine analysis of detailed guayulin content if proper calibration and validation procedures with data acquisition protocols are established.

The aim of the present study is the determination, for the first time, of the detailed content of guayulins A, B, C, and D of guayule dry biomass in addition to its rubber and resin content, using NIR spectroscopy and considering different approaches and ranges of wavelengths for obtaining the most robust and reliable PLSR model.

2. Materials and methods

2.1. Guayule samples

A set of 144 guayule samples were selected for the present study (Table 2). The guayule accessions were grown in Santa Cruz de la Zarza (Toledo, Spain) in three replicate plots. Plants were manually harvested by cutting them 5 cm above the ground and they were packaged into kraft bags, special care was taken to keep the time between harvesting, transport to the laboratory and drying to a minimum (4–6 h). Samples were dried in the laboratory for 48 h at 60 °C to achieve 12% moisture content. Moisture content of the samples was determined with an halogen lamp moisture balance model XM-120 T (Cobos, Barcelona, Spain) at 105 °C. When moisture loss was less than 0.1% in 180 s, it was considered that samples had reached constant mass. Then, leaves and flowers were manually removed and the dry biomass weight was calculated from the dried stems and leaves. Stems (30 g) were cut into pellets of about 1 cm in length with a manual cutter and were grounded in a 2-step procedure: first, 2 mm-sized particles were obtained using a hammer grinder (Mader 57075) for 10–15 s and then 0.5 mm-sized particles were obtained with a centrifuge grinder (Retsch ZM 1000) for 2 min. Dried ground samples were stored in screw cap closed glass vessels at room temperature.

2.2. NIR analysis

Approximately 2 g of each powdered guayule samples were placed into quartz sample plates of 3 cm diameter (Perkin-Elmer, Norwalk, USA), in case of liquid samples (resin and rubber extracts, and guayulins A and B standard solutions) 1 mL of sample was processed. Samples were analyzed by a Perkin Elmer Spectrum One FT-NIR equipment (Norwalk, USA) coupled with a near infrared reflectance accessory (NIRA). Data collection was acquired over a wavelength range of 750–2500 nm and the resolution was set at 16 cm^{-1}. All samples were scanned in duplicate.

Data processing: Multivariate analysis was used for quantitative and qualitative analysis. The tracking procedure of PLS modeling provided a systematic profile that combined different spectral pretreatment methods in order to suppress various adverse effects from physical properties of the sample, technical errors during measurements or, simply, the instrumental noise. The Spectrum-One software was used to perform data pretreatment and establish partial least squares regression (PLSR) models for studied contents. Spectra pretreatment combinations were carried out by using standard normal variate (SNV), smoothing (19, 25, and 37 points), de-trending (DT) and Savitzky–Golay first and second derivative (5, 9, and 13 points) preprocessing for all measurements to get the most robust model.

Model performance was evaluated using the root mean square error of calibration ($RMSEC = \left[\sum_{i=0}^{n}(f_i - y_i)^2/n\right]^{\frac{1}{2}}$; where yi represents the measured values and fi represents the predicted values), the coefficient of determination for calibration ($r_c^2 = \left[\left(\Sigma_i(y_i - f_i)^2\right)\Big/\left(\Sigma_i(y_i - \bar{y})^2\right)\right]$), and the residual predictive deviation ($RPD = [\text{Standard deviation of measured extracts}/RMSE]$; where RMSE is the root mean square error) as described by Luo et al. (2019).

During calibration development, cross-validation was used to select the optimal number of latent variables and minimize the equation overfitting. In addition to r^2, the ratio of standard deviation to standard error of cross-validation ($RPDc = SDcal/SECV$) was used to assess the overall quality of the fit obtained for each equation according to Suchat et al. (2013). The ratio of standard deviation to standard error of prediction (RPDp) was also calculated as $SDval/SEP$ (where SDval was the standard deviation of the validation samples) (Suchat et al., 2013).

2.3. Resin and rubber extraction

Sequential resin and rubber extraction was carried out in a Speed 139 Extractor BUCHI E-914 (Barcelona, Spain). A sample of 1.500 ± 0.005 g of guayule (0.51 mm-sized particles of guayule stems) was weighed and homogenized with approximately 32 g of sand as a dispersing agent and packed with 37 g of sand above and below to fill the stainless steel 80-cm^3 extraction cell, leaving 1-cm free upper space. A cellulose acetate filter was also placed at the top and bottom of each cell to avoid sample particles leaking into the cells. The resin extraction was carried out with acetone as solvent at 40 °C while rubber is extracted with hexane at 120 °C. Other parameters fixed in both extractionas were pressure 100 bar, hold 3 cycles 10/20/30 min, heat-up 1 min, discharge 3 min, flush with solvent 2 min and flush with N_2 5 min

Each extract (resin and rubber) independently was collected in a 240-cm^3 flask and transferred to a pre-weighed flask and equilibrated for 30 min in a desiccator. Solvent evaporation was carried out in a parallel Multivapor BUCHI P-6 system (Postfach, Switzerland) at 50 °C and 150 mbar. After evaporation, the pre-weighed flasks were maintained for 60 min in a desiccator before final weighing. The resin and rubber percentage were then determined gravimetrically considering the stem dry weight. Each sample was extracted twice.

Table 3
Descriptive statistic for resin and rubber fraction (gravimetric data) and guayulins A, B, C, and D (HPLC data).

Statistic parameters	Rubber (%)	Resin (%)	HPLC chromatogram areas at their max wavelength				Guayulins (g kg^{-1} dried plant)[a]	
			A	B	C	D	A	B
Minimum value	0.15	2.20	456.39	178.76	2348.91	893.47	0.05	0.05
Maximum value	6.79	13.33	48,957.40	8457.75	17,265.60	6326.26	16.26	13.09
Mean value	1.90	7.48	10,280.94	3211.79	7101.65	3345.55	2.53	3.68
Standard deviation	1.55	2.42	10,797.54	2640.78	3399.06	1488.51	3.25	3.68
Standard error	0.13	0.20	932.77	223.19	283.26	124.04	0.28	0.31

[a] Guayulins isolated in the laboratory.

2.4. Guayulin quantification by high-performance liquid chromatography–diode array detection

Twenty microliters of resin dissolved in ethanol (10 mg mL^{-1}) and filtered (0.22 μm) was injected into an Agilent 1200 high-performance liquid chromatography (HPLC) system (Agilent Technologies, Palo Alto, CA) equipped with a diode array detector (DAD) (Agilent Technologies, G1315D). Separation was performed at 30 °C on a reverse-phase ACE Excel 3 C18-PentaFluorPhenyl (PFP) column (150 × 4.6 mm, 3 μm particle size) protected with an ACE Excel HPLC Pre-column Filter (0.5 μm particle size) (both from Advanced Chromatography Technologies Ltd., Reading, Berkshire, UK). The solvents were Milli Q-grade water (solvent A) and acetonitrile (solvent B). The elution gradient for solvent B was as follows: 0 min, 60%; 10 min, 60%; 20 min, 80% and hold 5 min; 35 min, 100%, and hold 2 min

Guayulins A, B, C and D were tentatively identified by their characteristic UV absorption spectra (maximum at 256 nm for guayulins B and D, maximum at 276–278 nm for guayulin A and C) and retention time (Rozalén et al., 2021b).

Standards of guayulins A and B were isolated in the laboratory due to the lack of commercial standards. For this purpose, the low molecular weight guayule rubber (LMWGR) was removed from the resin extract (Zoeller et al., 1994). Then, free-rubber resin was fractionated using flash chromatography (VersaFlash Station System I equipped with a Versaflash cartridge, 23 mm × 110 mm, containing Spherical C18 bonded silica 30 g, 20–45 μm) with acetonitrile:water (80:20) as solvent and a flow rate of 20 cm^3 min^{-1}. The corresponding fraction for each guayulin was evaporated under vacuum and crystallized from hexane/chloroform as described by Martínez et al. (1986). Molecular weight and mass fragmentation patterns were confirmed by high-performance liquid chromatography coupled to mass spectrometry (LC-MS). Chromatographic purities were 93.2% at 276 nm for guayulin A, and 100% at 255 nm for guayulin B. Quantification of guayulins A and B was carried out from the corresponding calibration curve: guayulin A (1.25–2000 mg L^{-1}; $r^2 = 0.9997$; instrument detection limit (LOD): 0.024 ± 0.001 mg L^{-1}; Instrument quantification limit (LOQ): 0.080 ± 0.002 mg L^{-1}) and guayulin B (5–4000 mg L^{-1}; $r^2 = 0.9995$; LOD: 0.219 ± 0.000 mg L^{-1}; LOQ: 0.731 ± 0.000 mg L^{-1}).

3. Results and discussion

3.1. Rubber and resin extraction (ASE) and guayulin characterization data (HPLC) for guayule set of samples

The entire set of guayule samples (144) used for the present study were of different ages (up to 2 years old), accesions and even submitted to different agronomic practices, in order to get a more representative trial. The descriptive statistic data for both rubber and resin content, as well as for the detailed guayulins, are shown in Table 3.

The rubber content of the studied plants ranged from 0.15% to 6.79%, and their resin fraction between 2.20% and 13.33%. As plants were only 2 years old, the rubber content was still low and, which is expected to increase in the future up to a 8–10% whereas the resin content reached the usual range of variation for this extractible biomass component. Once resin fraction was extracted, the individual guayulins were quantified by HPLC-DAD, which was considered the reference standard method for their determination (Rozalén et al., 2021d; Spano et al., 2018). The quantification of individual guayulins A and B, using for each of them their corresponding calibration curve, showed that the majority guayulin was guayulin B with a mean content of 3.68 g kg^{-1} dried plant, followed by guayulin A with a mean concentration of 2.53 g kg^{-1} dried plant. Although guayulin C and D were quantified in terms of area at their respective maximum wavelength, the quantification in terms of mg kg^{-1} was not carried out as neither commercial standards nor sufficient purity standards from our lab trials were available.

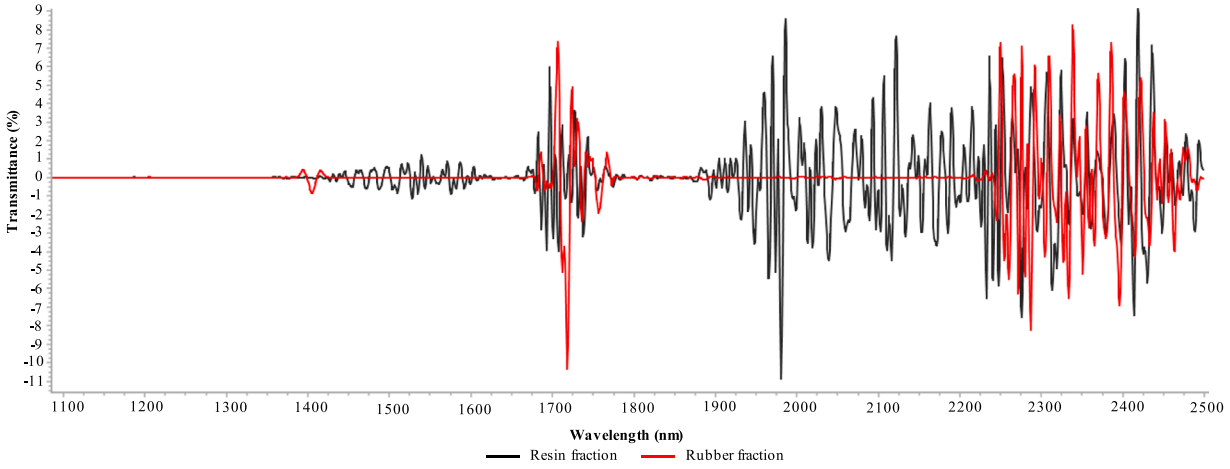

Fig. 1. NIR spectra obtained by direct measurement of a resin and rubber extract between 750 and 2500 nm.

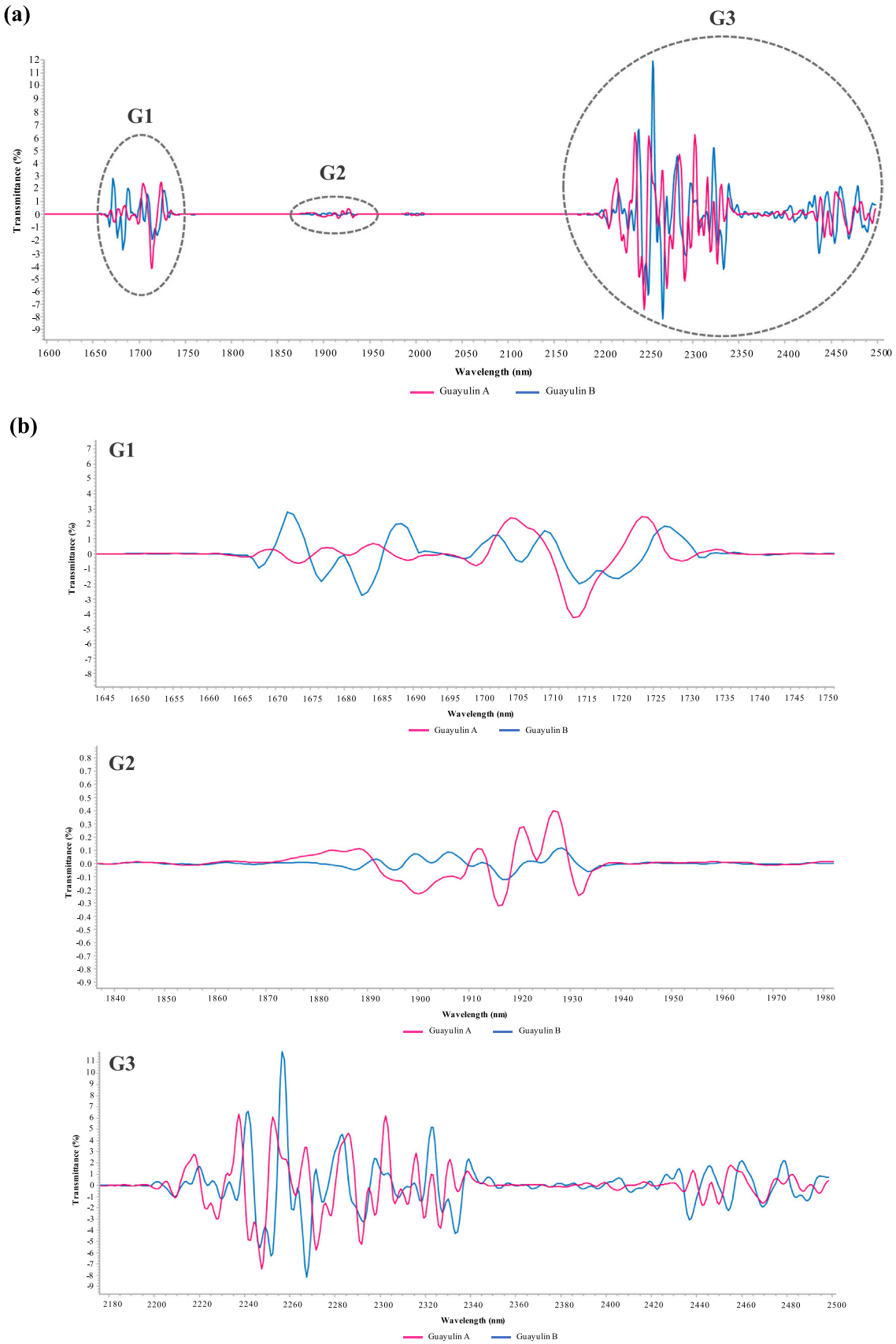

Fig. 2. (a) NIR spectra obtained when measuring the standards of guayulins A and B, (b) comparison between the spectra of guayulins A and B in the three absorption zones.

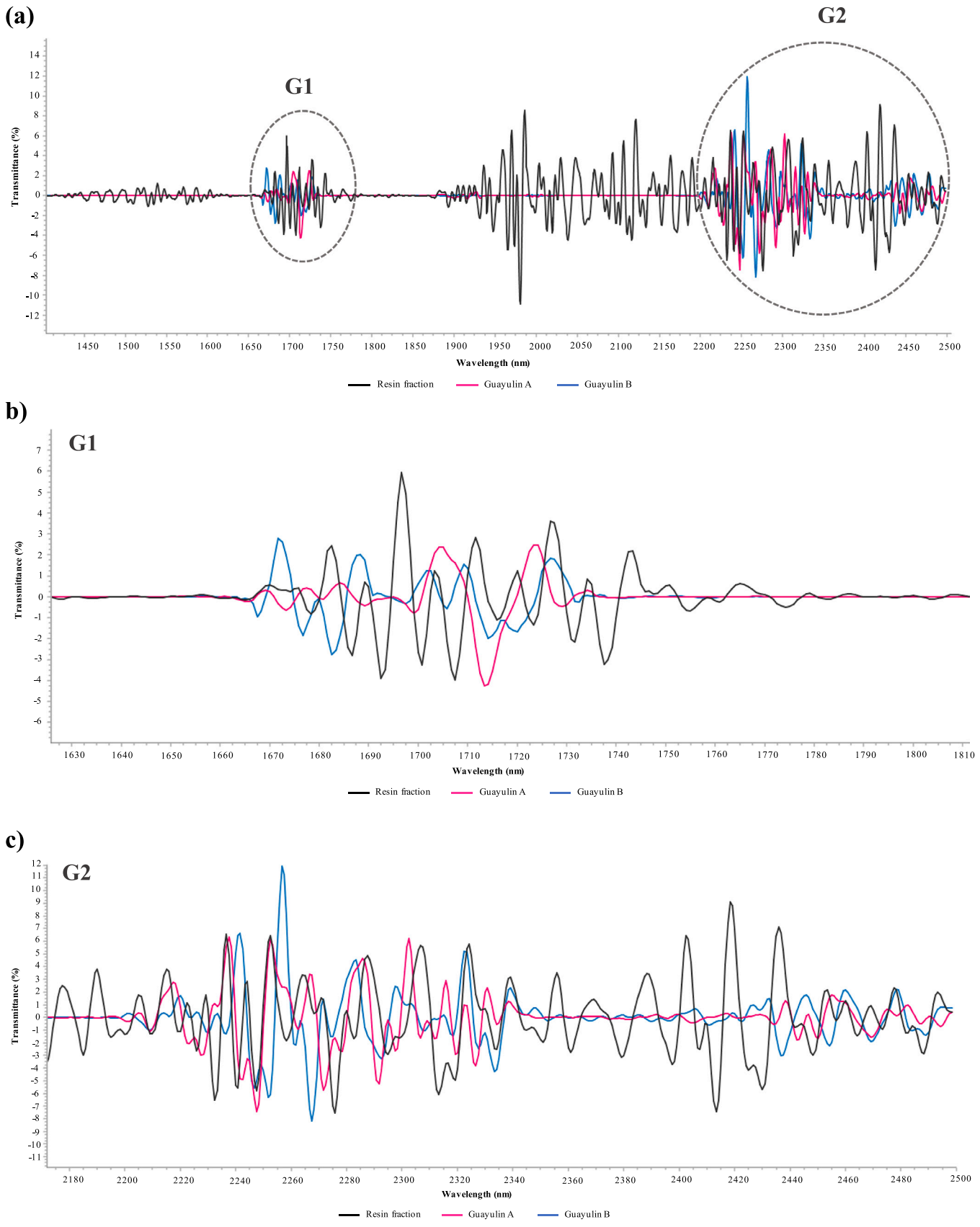

Fig. 3. (a) Superposition of the NIR spectra obtained by measuring between 750 and 2500 nm a resin extract and the standards of guayulins A and B, (b) detail of zone G1 and (c) detail of zone G2.

Table 4
NIR statistical parameters for the calibration data of the measured variables (% rubber, % resin and individual guayulins).

Statistic parameters	Rubber	Resin	Guayulins			
			A	B	C	D
r^2c[a]	0.97	0.92	1.00	1.00	0.96	1.00
RMSEC[b]	0.28	0.70	0.86	0.73	194.43	0.21
RPDc[c]	3.13	3.10	3.41	3.11	2.70	3.40

[a] r^2c: coefficient of determination for calibration;
[b] RMSEC: root mean squared error of calibration;
[c] RPDc: ratio performance to deviation. Calculated according to Suchat et al. (2013).

3.2. NIR interpretation for rubber and resin fractions and guayulin standards

Both ASE and HPLC-DAD are time-consuming, labor-intensive methods, and most important, they are not easily scaled-up to hundreds of samples (Rozalén et al., 2021a, 2021c; Salvucci et al., 2009; Spano et al., 2018; Suchat et al., 2013). Avoiding its use by employing the NIR technique for the estimation of any of the fractions or compounds present in guayule is a better option for routine analysis in time, as the measurement takes as little as 1 min per sample. According to previous works, the authors use different scanning ranges (Table 1), so in this sense the rubber and resin extracts have being fully scanned in the range of 750–2500 nm, in order to fine tune the scan to generate the best PLSR model.

All the samples show a similar spectrum (data not shown), with higher or lower absorbance and, in addition, this spectrum is similar to that obtained by other authors (Black et al., 1985; Luo et al., 2019). The overlay of the NIR spectra of the resin and rubber fractions between 750 and 2500 nm (Fig. 1) shows that the 1640–1800 nm wavelength region, which had previously been described as the first overtone of C–H stretching combination bands which can be attributed methyl and methylene bands that may be indicators of oligo- and polyterpenes and rubber molecules (Cornish et al., 2004). Between 1890 and 2250 nm, bands are due only to resin composition, as no bands are observed in the case of rubber which would inevitably include terpenoids and their derivatives, as the main fraction components.

The bands between 2250 and 2500 nm could be due to the combination of C-H stretching/strain caused by the surrounding molecules of rubber particles in guayule and other resin constituents such as guayulins (Fig2a). The best correlative PLSR models for rubber and resin extract were developed within the range of 1100–2500 nm.

The overlay of the NIR spectra of the guayulins A and B standards (Fig. 2a) show three clearly separated absorption regions that are common to both guayulins (Fig. 2b). Comparing these regions in detail, it is observed that the spectra are very similar, especially in the third absorption region.

As previously commented, guayule resin contains sesquiterpene esters (guayulins), triterpenoid esters (argentatins A-H) and polyphenols (tannins and flavonoids) as well as triglycerides of fatty acids, lipids, pigments, and other acetone-soluble materials (Cheng et al., 2020; Dehghanizadeh et al., 2020; Jara et al., 2019; Salvucci et al., 2009). If NIR spectra of both resin and guayulin standards (A and B) are overlayed (Fig. 3), it can then be observed which are the characteristic absorption bands of sesquiterpene esters within the resin fraction, as well as those corresponding to other types of elements still to be identified, which would correspond to bands between 1440 and 1610 nm and 1940–2190 nm.

3.3. NIR calibration and validation

The best fitted models indicated the efficiency of SNV in removing multiplicative interferences of scattering and particle size, selecting Savitzky–Golay first derivative (5 points) for improving deconvolution of some overlapping spectral peaks to unveil hidden information under these peaks. Reliable models have also been constructed when the combinations of all or part of the two pre-processing approaches (i.e. SNV and second derivative) were used in previous guayule studies (Luo et al., 2019). As for the PLSR calibration performed for the rubber and resin content (Table 4), it showed an excellent correlation with the values estimated by the NIR calibration ($r^2c = 0.97$ in the case of rubber and 0.92 in the case of resin). The low RMSEC values are good indicators of the good accuracy of the selected model. Comparing the rubber and resin results obtained with those of Suchat et al. (2013), the RPDc parameter was lower than the obtained by them. Perhaps this may be due to the fact that their determination coefficients for calibration were higher than those obtained in this test.

Considering the guayulins, excellent r^2c values were obtained (Table 4), with the highest RPDc values resulting for guayulins A and D, and no comparison can be carried out as no references have been found in the bibliography.

Cross-validation (CV) was used for the evaluation of the PLSR results and the statistical parameters are shown in Table 5. A higher RPD value demonstrates higher predictive power of the model, with values above 2.0 being applicable to approximate screening and RPD above 3.0 can be interpreted as good in the control quality of NIR models (Luo et al., 2019), and thus applied with confidence on a routine basis. In the case of the rubber and resin fractions, the r^2cv values of 0.90 were positive values and even better than those obtained by other authors (Table 1), which is confirmed by their high RPD, 3.22 and 3.18, respectively.

In the case of guayulins, very good r^2cv values between 0.87 and 0.92 were obtained, the highest values being obtained for guayulins A and D. As for the RMSECV values, these were higher for guayulins A and B compared with guayulins C and D. The residual predictive deviation (RPD) was higher than 3 for guayulins A, B, and D, while for guayulin C it was 2.8. These high RPD values demonstrated the good predictive power of the model (Luo et al., 2019).

The previously reported resin RPD, Table 1, were higher than those of Luo et al. (2019) (2.05–2.41) and lower than those reported by Suchat et al. (2013) (4.23). As for the rubber fraction, the RPD values obtained by other authors (Table 1) were 5.28 in the case of Suchat et al. (2013) and ranged between 2.02 and 2.13 in different guayule samples reported by Luo et al. (2019). If these results are compared with those obtained in this study, they were lower than the ones obtained by Suchat et al. (2013) but higher than those of Luo et al. (2019).

Fig. 4 shows the scatter plots of the rubber and resin values obtained by ASE extraction versus the values predicted by NIR. Regression between the laboratory values and those predicted by NIR (Fig. 4) also led to a good correlation (0.97, rubber fraction; 0.92, resin fraction). The differences between rubber and resin in all cases are probably due to the fact that resin contains a wide range of different biochemical molecules, in contrast to the rubber fraction, which is essentially composed by a

Table 5
NIR statistical parameters for the validation data of the measured variables (% rubber, % resin and individual guayulins).

Statistic parameters	Rubber	Resin	Guayulins			
			A	B	C	D
r^2cv[a]	0.90	0.90	0.92	0.90	0.87	0.92
RMSECV[b]	0.48	0.76	878.64	1110.16	371.54	187.22
RPDp[c]	2.65	2.58	2.48	2.37	1.81	2.10
RPD[d]	3.22	3.18	3.70	3.32	2.80	3.53

[a] r^2cv: coefficient of determination for cross validation;
[b] RMSECV: root mean squared error of cross validation;
[c] RPDp: ratio performance to deviation for prediction. Calculated according to Suchat et al. (2013);
[d] RPD: residual predictive deviation. Calculated according to Luo et al. (2019).

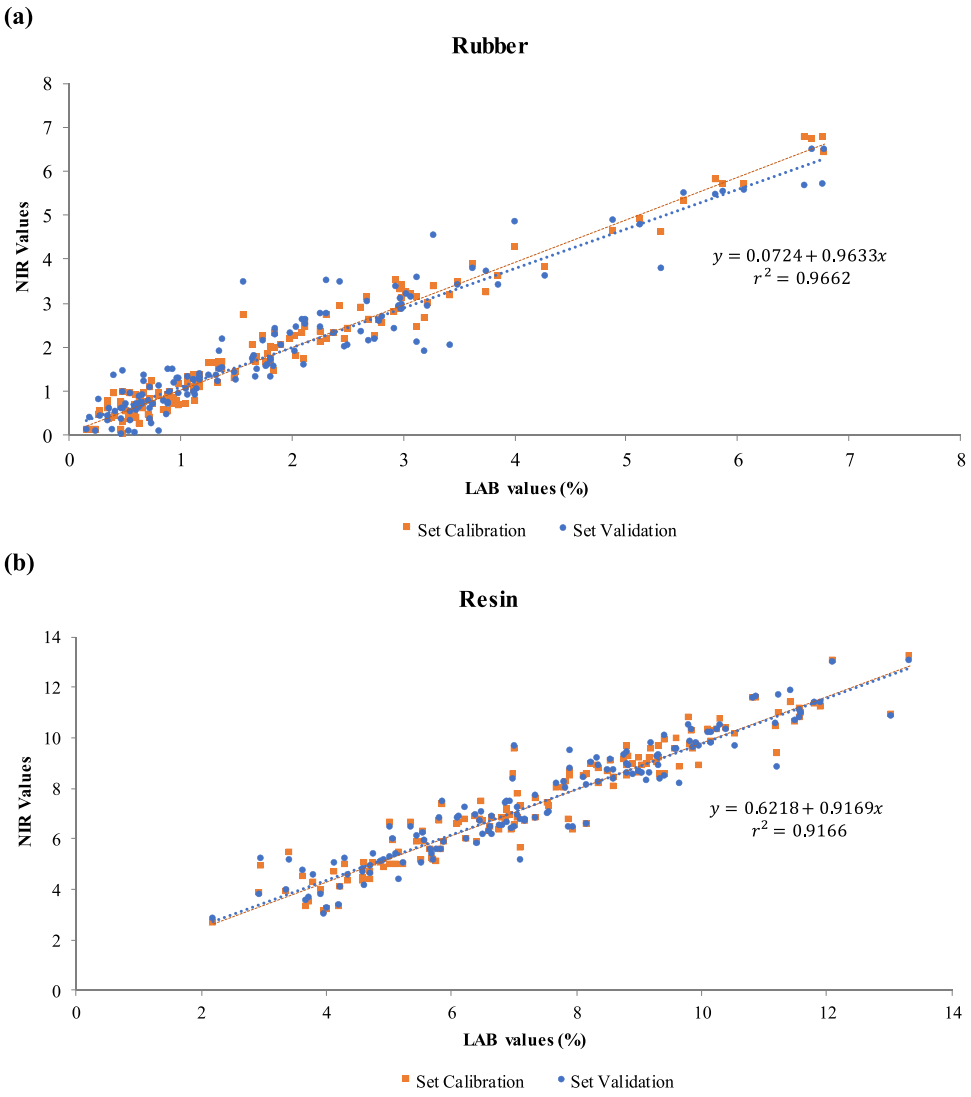

Fig. 4. Scatter plot of (a) rubber and (b) resin values obtained in the laboratory versus values predicted by the NIR.

single type of polymer.

On the other hand, Fig. 5 shows the content of guayulins A and B obtained by HPLC-DAD versus those predicted by NIR. In this case, very good correlations between laboratory values and those predicted by NIR were also obtained, being 0.96 for guayulin A and 0.95 for guayulin B.

4. Conclusions

Reliable PLSR models have been successfully constructed for the determination of resin, rubber and guayulins A and B content; as well as for the estimation of guayulins C and D in terms of chromatogram areas at their respective maximum wavelength, of dried and ground guayule biomass using near infrared spectroscopy (NIR).

The predicted residual deviation (RPD) was above 3 for resin, rubber, and guayulins A, B and D, while for guayulin C it was 2.8. These high RPD values demonstrated a good predictive power of the model, since with values above 2 it can be applied for approximate screening, and when RPD is above 3 it can be interpreted as a good control quality NIR model.

Thus, the use of NIR spectroscopy for the estimation of guayule resin and rubber, as well as guayulins has indeed proved to be a very good option for routine analysis as opposed to traditional time-consuming and labor-intensive techniques.

Funding

This work was supported through the Ramón y Cajal Fellowships [RyC-2014–16307] and the grant RTI2018–098042-B100 funded by MCIN/AEI/ 10.13039/501100011033; and through the project SBPLY-19–180501–00074 cofinanced by Junta de Comunidades de Castilla-La Mancha and the European Regional Development Fund. Guayente Latorre acknowledges a predoctoral contract (PREDUCLM-16215) from Universidad de Castilla-La Mancha and the European Social Fund.

CRediT authorship contribution statement

M. Mercedes García: Investigation, Writing. **Guayente Latorre**: Investigation, Visualization. **Francisco M. Jara**: Investigation. **Juana Rozalén:** Investigation, Visualization. **M. Engracia Carrión**: Writing – review & editing. **Manuel Carmona:** Methodology, Supervision, Writing – review & editing, Project administration. **Amaya Zalacain**: Conceptualization, Methodology, Validation, Visualization, Writing – review & editing, Project administration.

Declaration of Competing Interest

The authors declare that they have no known competing financial interests or personal relationships that could have appeared to influence

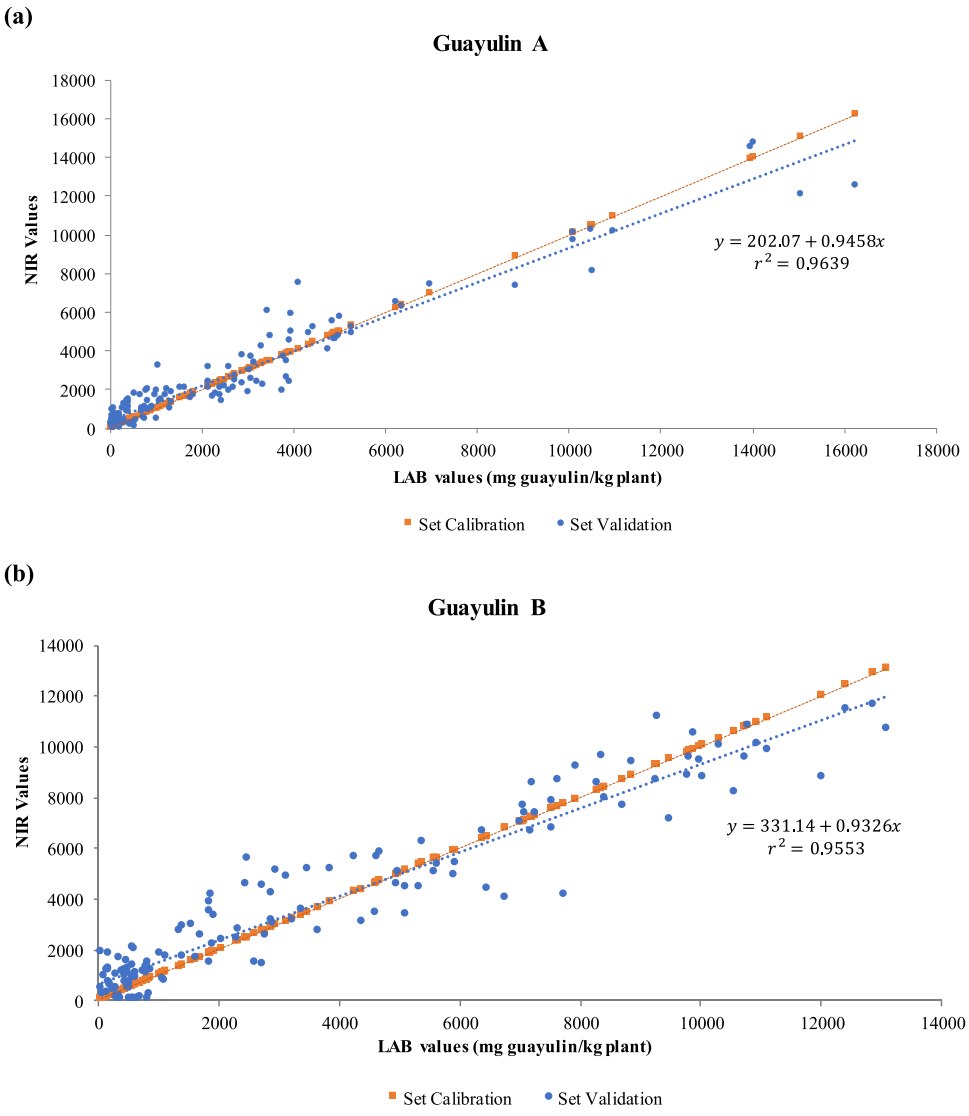

Fig. 5. Scatter plot of guayulins (a) A and (b) B values obtained in the laboratory versus NIR predicted values.

the work reported in this paper.

Acknowledgments

The authors wish to thank Agroservicios Guayule S.L. and Nokian Tyres Plc. for their support in this research.

References

Angulo-Sánchez, J.L., Neira-Velazquez, G., Jasso De Rodriguez, D., 1995. Multimodal molecular weight distributions of guayule rubber from high rubber yielding lines. Ind. Crops Prod. 4, 113–120 https://doi.org/doi.org/10.1016/0926-6690(95)00023-6.

Banigan, T.F., Verbiscar, A.J., Weber, C.W., 1982. Composition of guayule leaves, seed, and wood. J. Agric. Food Chem. 30, 427–431. https://doi.org/10.1021/jf00111a004.

Black, L.T., Hamerstrand, G.E., Kwolek, W.F., 1985. Analysis of rubber, resin, and moisture content of guayule by near infrared reflectance spectroscopy. Rubber Chem. Technol. 58, 304–313 https://doi.org/doi.org/10.5254/1.3536068.

Bultman, J.D., Gilbertson, R.L., Adaskaveg, J., Amburgey, T.L., Parikh, S.V., Bailey, C.A., 1991. The efficacy of guayule resin as a pesticide. Bioresour. Technol. 35, 197–201. https://doi.org/10.1016/0960-8524(91)90030-N.

Cheng, F., Dehghanizadeh, M., Audu, M.A., Jarvis, J.M., Holguin, F.O., Brewer, C.E., 2020. Characterization and evaluation of guayule processing residues as potential feedstock for biofuel and chemical production. Ind. Crops Prod. 150, 112311 https://doi.org/10.1016/j.indcrop.2020.112311.

Coffelt, T.A., Nakayama, F.S., Ray, D.T., Cornish, K., McMahan, C.M., 2009. Post-harvest storage effects on guayule latex, rubber, and resin contents and yields. Ind. Crops Prod. 29, 326–335. https://doi.org/10.1016/j.indcrop.2008.06.003.

Coffelt, T.A., Williams, C.F., 2009. Characterization and recycling of waste water from guayule latex extraction. Ind. Crops Prod. 29, 648–653. https://doi.org/10.1016/j.indcrop.2008.10.004.

Cornish, K., Myers, M.D., Kelley, S.S., 2004. Latex quantification in homogenate and purified latex samples from various plant species using near infrared reflectance spectroscopy. Ind. Crops Prod. 19, 283–296. https://doi.org/10.1016/j.indcrop.2003.10.009.

Cornish, K., Pearson, C.H., Rath, D.J., 2013. Accurate quantification of guayule resin and rubber requires sample drying below a critical temperature threshold. Ind. Crops Prod. 41, 158–164. https://doi.org/10.1016/j.indcrop.2012.04.014.

Dehghanizadeh, M., Cheng, F., Jarvis, J.M., Holguin, F.O., Brewer, C.E., 2020. Characterization of resin extracted from guayule (*Parthenium argentatum*): A dataset including GC–MS and FT-ICR MS. Data Br. 31, 105989 https://doi.org/10.1016/j.dib.2020.105989.

Dehghanizadeh, M., Mendoza Moreno, P., Sproul, E., Bayat, H., Quinn, J.C., Brewer, C.E., 2021. Guayule (*Parthenium argentatum*) resin: A review of chemistry, extraction techniques, and applications. Ind. Crops Prod. 165, 113410 https://doi.org/10.1016/j.indcrop.2021.113410.

Jara, F.M., Cornish, K., Carmona, M., 2019. Potential applications of guayulins to improve feasibility of guayule cultivation. Agronomy 9, 1–11. https://doi.org/10.3390/agronomy9120804.

Luo, Z., Thorp, K.R., Abdel-Haleem, H., 2019. A high-throughput quantification of resin and rubber contents in *Parthenium argentatum* using near-infrared (NIR) spectroscopy. Plant Methods 15, 1–14. https://doi.org/10.1186/s13007-019-0544-3.

Maatooq, G.T., 2002. Microbial conversion of partheniol by *Calonectria decora*. Zeitschrift fur Naturforsch. Sect. C. J. Biosci. 57, 680–685. https://doi.org/10.1515/znc-2002-7-822.

Maatooq, G.T., Hoffmann, J.J., 1996. Fungistatic sesquiterpenoids from *Pharthenium*. Phytochemistry 43, 67–69.

Martínez, M., Flores, G.A., Romo, A., Reynolds, G., Rodriguez, E., 1986. Guayulins C and D from Guayule (*Parthenium argentatum*). J. Nat. Prod. 49, 1102–1103. https://doi.org/10.1021/np50048a022.

McMahan, C.M., Cornish, K., Coffelt, T.A., Nakayama, F.S., McCoy, R.G., Brichta, J.L., Ray, D.T., 2006. Post-harvest storage effects on guayule latex quality from agronomic trials. Ind. Crops Prod. 24, 321–328. https://doi.org/10.1016/j.indcrop.2006.06.002.

Nakayama, F.S., Vinyard, S.H., Chow, P., Bajwa, D.S., Youngquist, J.A., Muehl, J.H., Krzysik, A.M., 2001. Guayule as a wood preservative. Ind. Crops Prod. 14, 105–111. https://doi.org/10.1016/S0926-6690(00)00093-5.

Romo de Vivar, A., Martínez-Vázquez, M., Matsubara, C., Pérez-Sánchez, G., Joseph-Nathan, P., 1990. Triterpenes in *Parthenium argentatum*, structures of argentatins C and D. Phytochemistry 29, 915–918 https://doi.org/doi.org/10.1016/0031-9422(90)80045-I.

Rozalén, J., García-Martínez, M.M., Carrión, M.E., Carmona, M., López-Córcoles, H., Cornish, K., Zalacain, A., 2021a. Adapting the accelerated solvent extraction method for resin and rubber determination in guayule using the Bücchi speed extractor. Molecules 26, 183. https://doi.org/10.3390/molecules26010183.

Rozalén, J., García-Martínez, M.M., Carrión, M.E., Zalacain, A., López-Córcoles, H., Carmona, M., 2021b. Guayulin content in guayule (*Parthenium argentatum Gray*) along the growth cycle. Ind. Crops Prod. 170, 113829 https://doi.org/10.1016/j.indcrop.2021.113829.

Rozalén, J., García-Martínez, M.M., Carrión, M.E., Zalacain, A., López-Córcoles, H., Carmona, M., 2021c. Effect of seasonal decrease in temperature on the content and composition of guayulins in stems of guayule (*Parthenium argentatum, Gray*). Plants 10, 537. https://doi.org/10.3390/plants10030537.

Rozalén, J., García-Martínez, M.M., Zalacain, A., López-Córcoles, H., Hurtado de Mendoza, J., Cornish, K., Carmona, M., 2021d. Future trends for the analysis of guayulins in guayule (*Parthenium argentatum Gray*) resins. Ind. Crops Prod. 159. https://doi.org/10.1016/j.indcrop.2020.113027.

Salvucci, M.E., Coffelt, T.A., Cornish, K., 2009. Improved methods for extraction and quantification of resin and rubber from guayule. Ind. Crops Prod. 30, 9–16. https://doi.org/10.1016/j.indcrop.2008.12.006.

Schloman, W.W., Bennett, D.J., Garrot, D.J., Ray, D.T., 1986. Seasonal effects on guayule resin composition. J. Agric. Food Chem. 34, 177–179. https://doi.org/10.1021/jf00068a005.

Schloman, W.W., Hively, R.A., Krishen, A., Andrews, A.M., 1983. Guayule byproduct evaluation: Extract characterization. J. Agric. Food Chem. 31, 873–876. https://doi.org/10.1021/jf00118a050.

Schloman, W.W., Mclntyre, D., Hilton, A.S., 1996. Effects of environment and composition on degradation of guayule rubber. J. Appl. Polym. Sci. 60, 1015–1023.

Spano, N., Meloni, P., Idda, I., Mariani, A., Itria Pilo, M., Marina, V., Izabela Lachowicz, J., Rivera, E., Orona-Espino, A., 2018. Assessment, validation and application to real samples of a RP-HPLC method for the determination of guayulins A, B, C and D in guayule shrub. Separations 5, 23. https://doi.org/10.20944/preprints201802.0161.v2.

Suchat, S., Pioch, D., Palu, S., Tardan, E., van Loo, E.N., Davrieux, F., 2013. Fast determination of the resin and rubber content in *Parthenium argentatum* biomass using near infrared spectroscopy. Ind. Crops Prod. 45, 44–51. https://doi.org/10.1016/j.indcrop.2012.09.025.

Taurines, M., Brancheriau, L., Palu, S., Pioch, D., Tardan, E., Boutahar, N., Sartre, P., Meunier, F., 2019. Determination of natural rubber and resin content of guayule fresh biomass by near infrared spectroscopy. Ind. Crops Prod. 134, 177–184. https://doi.org/10.1016/j.indcrop.2019.03.073.

Teetor, V.H., Ray, D.T., Schloman, W.W., 2009. Evaluating chemical indices of guayule rubber content: Guayulins A and B. Ind. Crops Prod. 29, 590–598. https://doi.org/10.1016/j.indcrop.2008.11.005.

Wang, Y., Xiang, J., Tang, Y., Chen, W., Xu, Y., 2021. A review of the application of near-infrared spectroscopy (NIRS) in forestry. Appl. Spectrosc. Rev. https://doi.org/10.1080/05704928.2021.1875481.

Xiao, L., Wei, H., Himmel, M.E., Jameel, H., Kelley, S.S., 2014. NIR and Py-mbms coupled with multivariate data analysis as a high-throughput biomass characterization technique: A review. Front. Plant Sci. 5, 1–10. https://doi.org/10.3389/fpls.2014.00388.

Zhao, N., Wu, Z.S., Zhang, Q., Shi, X.Y., Ma, Q., Qiao, Y.J., 2015. Optimization of parameter selection for partial least squares model development. Sci. Rep. 5, 1–10. https://doi.org/10.1038/srep11647.

Zoeller, J., Wagner, J.P., Sulikowski, G.A., 1994. Concise multigram purification of guayulin A from guayule. J. Agric. Food Chem. 42, 1647–1649. https://doi.org/10.1021/jf00044a012.